

MCTSteg: A Monte Carlo Tree Search-based Reinforcement Learning Framework for Universal Non-additive Steganography

Xianbo Mo, *Student Member, IEEE*, Shunquan Tan*, *Senior Member, IEEE*, Bin Li, *Senior Member, IEEE*, and Jiwu Huang, *Fellow, IEEE*

Abstract—Recent research has shown that non-additive image steganographic frameworks effectively improve security performance through adjusting distortion distribution. However, as far as we know, all of the existing non-additive proposals are based on handcrafted policies, and can only be applied to a specific image domain, which heavily prevent non-additive steganography from releasing its full potentiality. In this paper, we propose an automatic non-additive steganographic distortion learning framework called MCTSteg to remove the above restrictions. Guided by the reinforcement learning paradigm, we combine Monte Carlo Tree Search (MCTS) and steganalyzer-based environmental model to build MCTSteg. MCTS makes sequential decisions to adjust distortion distribution without human intervention. Our proposed environmental model is used to obtain feedbacks from each decision. Due to its self-learning characteristic and domain-independent reward function, MCTSteg has become the first reported universal non-additive steganographic framework which can work in both spatial and JPEG domains. Extensive experimental results show that MCTSteg can effectively withstand the detection of both hand-crafted feature-based and deep-learning-based steganalyzers. In both spatial and JPEG domains, the security performance of MCTSteg steadily outperforms the state of the art by a clear margin under different scenarios.

Index Terms—Steganography, Steganalysis, Monte Carlo Tree Search, Reinforcement Learning

I. INTRODUCTION

STEGANOGRAPHY hides secret information into stego media and try to evade detection from steganalysis, where spatial and JPEG domain images are the most common cover media [1]. Almost all modern steganographic algorithms are based on a distortion minimization framework [2], decomposing a steganographic algorithm into the design of cost function and coding scheme. When we study

S. Tan is with College of Computer Science and Software Engineering, Shenzhen University. X. Mo, B. Li, and J. Huang are with College of Information Engineering, Shenzhen University.

All of the members are with the Guangdong Key Laboratory of Intelligent Information Processing, Shenzhen Key Laboratory of Media Security, Guangdong Laboratory of Artificial Intelligence and Digital Economy (SZ), Shenzhen Institute of Artificial Intelligence and Robotics for Society, China(email: tansq@szu.edu.cn).

*S. Tan is the correspondence author.

This work was supported in part by the Key-Area Research and Development Program of Guangdong Province (2019B010139003), NSFC (61772349, U19B2022, 61872244), Guangdong Basic and Applied Basic Research Foundation (2019B151502001), and Shenzhen R&D Program (JCYJ20180305124325555). This work was also supported by Alibaba Group through Alibaba Innovative Research (AIR) Program.

the cost function, the optimal embedding simulator can be used to simulate real embedding impact. Started by Pevný and Filler [3], several heuristic cost functions such as [4]–[9] have been proposed.

These algorithms attain global distortion by summing up the local costs of individual pixels and thus were called *additive steganography*. However, the application of content-adaptive cost function causes embedding modifications clustering in textured areas, so inter-pixel correlations and interactions among these modifications destroy the prerequisite for additive distortion. Filler and Fridrich [10] introduced *non-additive steganography* in the spatial domain. Later, distortion adjustment strategies were proposed to guide the direction of embedding modifications. In CMD [11] and Synch [12], the authors pointed out that clustering modification directions are helpful to improve security performance. In the JPEG domain, Li et al. [13] proposed a strategy called BBC to maintain the block boundary continuity. Wang et al. [14] first developed a non-additive framework called BBC++ based on BBC and then proposed BBM [15] to minimize the modifications on the spatial block boundaries, which can be combined with BBC. As for coding schemes [16]–[18], STC is the most commonly used one for practical application. Recently, based on polar codes, Zhang et al. [19] proposed a better near-optimal steganographic coding method called SPC.

Steganalysis detects secret bits hidden in cover media. The most well-known traditional steganalyzers are the “rich models” [20]–[24], a hand-crafted feature family, equipped with ensemble classifier [25]. Recently, this battleground has been dominated by deep learning frameworks. Based on auto-encoders, Tan and Li [26] made the first attempt, and then Xu et al. [27] proposed a deep learning-based network with convolutional and linear layers, which is a milestone in steganalysis networks. Later, deeper and more complex structures [28]–[33] were proposed for either spatial- or JPEG-domain by exploiting background knowledge of hand-crafted feature based steganalysis. Boroumand et al. [34] proposed SRNet, a domain-independent deep residual network with superior detection performance, whose objective is minimizing the use of heuristic domain knowledge. Tan et al. [35] proposed CALPA-NET, a channel pruning-assisted deep residual network architecture to shrink the size of

existing vast and over-parameterized deep learning-based steganalyzers.

Meanwhile, deep learning structure has also been applied in steganographic methods. ASDL-GAN [36] and UT-GAN [37] are the most representative deep learning-based steganographic frameworks. Both ASDL-GAN and UT-GAN are composed of two subnetworks, the first one is steganographic generative subnetwork, which aims at learning embedding probabilities. The second one is steganalysis discriminative subnetwork, which tries to distinguish whether the input is cover or stego. Moreover, based on the reinforcement learning paradigm, Tang et al. [38] proposed Steganographic Pixel-wise Actions and Rewards with Reinforcement Learning (SPAR-RL), which aims at maximizing the rewards evaluated by the steganalysis environment. Please note that, all these three mentioned frameworks are additive steganographic framework, thus their security performance is far behind non-additive steganographic frameworks. But, on the other hand, there are defects in current non-additive steganography [11]–[15]. For example, all of them are based on handcrafted distortion adjustment strategies. Furthermore, these strategies are designed for specific domain, implying that they can only work in either spatial or JPEG domain.

In this paper, we develop a novel universal non-additive steganographic framework called *MCTSteg*, aiming at automatically adjusting distortion without human intervention. This framework is inspired by the huge success of the AlphaGo family [39], [40], the first computer program to defeat a professional human Go player, because we think there are similarities between Go and non-additive steganography. For steganographers, they modify cover media by ± 1 in least-significant-bit (LSB) plane to transmit secret message. Specially, in non-additive steganography, steganographers control the location distribution of ± 1 modifications by adjusting embedding distortion, which is similar to put down black and white pieces on a Go board. As the core component of AlphaGo infrastructure, the Monte Carlo Tree Search (MCTS), a robust machine learning method, is utilized to find optimal solutions in given space by building a search tree. Therefore, we adopt MCTS tree into our framework. From the respect of game theory, *MCTSteg* is composed of two modules, where the deep learning-based steganalyzer acts as environmental model and MCTS tree acts as non-additive steganographer. Guided by background knowledge, we define the reinforcement learning elements to connect MCTS and steganography. To win the battle between steganographer and steganalyzer, *MCTSteg* first divides the cover image into several sublattices. For each sublattice, its distortion distribution of different modification polarities is adjusted according to the search result of MCTS without any non-additive steganographic rules. For the adjustment order, we design a new distortion-adaptive strategy called *distortion descending order (DDO)*. Next, we design a reward function to calculate feedbacks of each decision made by *MCTSteg*. Because the reward function can work in both spatial and JPEG domain, *MCTSteg* is a native universal framework.

After executing enough searches, *MCTSteg* can learn to generate more secure embedding distortion. Extensive experiments conducted on three datasets with the optimal embedding simulator show that under the detection of both hand-crafted feature-based and deep learning-based steganalyzers, stego images generated by *MCTSteg* achieve the best statistical score and security performance compared with state-of-the-art non-additive steganographic frameworks and machine learning-based steganography.

The rest of this paper is organized as follows. In Sect. II, we make a brief overview of the preliminaries in our research. Then we describe the technical roadmap and challenges of *MCTSteg* in Sect. III. To demonstrate the effectiveness of our framework, Sect. IV first presents experimental setup and statistical analysis. Next, it compares security performance against various steganalyzers with state-of-the-art steganographic methods. Finally, we conclude and list our future work in Sect. V.

II. PRELIMINARIES

A. Non-additive Steganographic Framework

Started by Filler and Fridrich, they proposed the Gibbs construction framework [10] which consists of four steps. Firstly, local potentials are calculated by the cost function so that the distortion minimization framework can be employed. The distortion D that cover C changes into stego S is expressed as:

$$D(C, S) = \sum_{i=1}^N \sum_{j=1}^N [\rho_{i,j}^+ \delta(d_{i,j} - 1) + \rho_{i,j}^- \delta(d_{i,j} + 1)], \quad (1)$$

where ρ^+ and ρ^- are the distortions that $c_{i,j}$ modifies by +1 and -1 respectively; $d_{i,j}$ represents the difference between the stego and the cover; $\delta(\cdot)$ is an indicator function:

$$\delta(x) = \begin{cases} 1 & x = 0 \\ 0 & x \neq 0. \end{cases} \quad (2)$$

Secondly, the cover image is decomposed into disjoint sublattices with a distance larger than the support width of local potential. Specially, in JPEG-domain, sublattices are divided based on 8×8 DCT block. Thirdly, in each iteration, one sublattice is embedded while the distortion of others are updated. Finally, the iterations are repeated until convergence, and the introduced embedding pattern is expected to be a sample from optimal embedding.

Prior research, including CMD [11] and Synch [12], has demonstrated that based on the additive cost function, synchronizing the direction of embedding modification improves security performance with a small entropy of stego noise. In CMD, modification synchronization is achieved by adjusting the distortion contribution as:

$$\rho_{i,j}^+ = \begin{cases} \rho_{i,j}^+/\alpha & \text{If nearby modification is more than } +1 \\ \rho_{i,j}^+ & \text{otherwise} \end{cases} \quad (3)$$

$$\rho_{i,j}^- = \begin{cases} \rho_{i,j}^-/\alpha & \text{If nearby modification is less than } -1 \\ \rho_{i,j}^- & \text{otherwise,} \end{cases} \quad (4)$$

where α is a scaling factor. A larger α leads to a more concentrated embedding direction.

B. Monte Carlo Tree Search

When we face the challenge of tremendous search space dimensionality such as Go, MCTS is always robust to make the optimal decisions by building an MCTS tree with its search results. The whole procedure is composed of four stages:

- 1) *Selection*: Starting from the root node, the selection direction is guided by the tree policy. Each time only one node is chosen from the available child node set. During the whole search process, the visiting counts of all selected nodes are increased by one. Finally, if a fully expanded node is not reached, the search procedure goes to *expansion*. If a leaf node is reached, the search procedure goes to *backpropagation*.
- 2) *Expansion*: An unvisited child node is randomly selected and added to the MCTS tree. Then it goes to *simulation*.
- 3) *Simulation*: A default policy such as random search guides the child node selection and updates parameters until a leaf node is reached. Thus the search result is obtained, and the search procedure goes to *backpropagation*.
- 4) *Backpropagation*: The reward or penalty feedback of the search result is calculated and added to the cumulative reward of each selected node in the search path.

The most popular *tree policy* is *Upper Confidence Bound for Trees* [41, UCT]. Let v denote a child node and v' be its parent. The UCT score of v is calculated by:

$$\text{UCTScore}(v) = \frac{R(v)}{N(v)} + C \sqrt{\frac{\ln N(v)}{N(v')}}, \quad (5)$$

where $R(\cdot)$ represents the cumulative reward, $N(\cdot)$ is the visiting count. The two terms in this equation make a balance between exploration and experience where C is a weighting factor. As a strategy, UCT selects the node with the maximum UCT score. However, it relies on the statistics of visited nodes, which means that it cannot be applied to unvisited nodes. Therefore, in *expansion* and *simulation*, random selection is adopted as the default policy. With a lower complexity, the search procedure can be executed faster so that more results can be generated in a limited time.

C. Reinforcement Learning

Reinforcement learning is a self-learning algorithm and can be used to develop game strategies through continuous interaction between players and environments. To model the real scenario, reinforcement learning contains the following basic elements:

- S : A set of states, where s^0 denotes the initial state and s^T denotes the terminal state.
- A : A set of actions. For each $s^i \in S$, an action a is sampled from A and transfer s^i to s^{i+1} .
- $f(s, a, s')$: A function that denotes the transfer from s to s' with action a .
- π : A policy π is a probability distribution that guides the action selection.
- $R(s^i, a, s^{i+1})$: The reward value of selecting action a at state s_i .
- E : An environmental model for evaluating s^T .

As a game-like situation, players have to make a series of decisions from s^0 to s^T based on π . Then R is calculated by E and assigned to all related actions. The goal of reinforcement learning is to achieve the maximum total reward. In Sect. III, we present more details of reinforcement learning elements used in our proposed framework.

III. PROPOSED FRAMEWORK

A. Technical Roadmap and Challenges

In game theory, most games can be modeled by basic elements including players, environmental models, states, actions, and rewards. Taking Go as an example, starting from the initial state of a blank Go board, players elaborately take actions until the result is settled down according to Go rules which can be seen as an environmental model.

For the game between non-additive steganographer and steganalyzer, the embedding distortion calculated by the additive cost function is our initial state. To win this game, the non-additive steganographer takes a series of actions to adjust the distortion distribution. Then stego images are generated according to the adjusted distortion, and the steganalyzer classifies these images. If the steganalyzer gives a wrong prediction, the steganographer wins this game. Otherwise, the steganographer loses. Therefore, this well-trained steganalyzer acts as an environmental model. As we all know, MCTS is a wise decision-maker [42], but it is doubtful whether MCTS can be a good steganographer without human guidance. To address this issue, we build an MCTS-based non-additive steganographic framework. There are three major challenges:

- 1) *Relevance*: MCTS is a tool for making decisions in a search space, while steganography is an information hiding technique. It is difficult to combine the search space of MCTS with the distortion metric of the distortion minimization framework.
- 2) *Game Rules*: In most games such as Go and Chess, the game rules are clearly defined, so the game results can be easily obtained. In steganography, there are no such rules available.

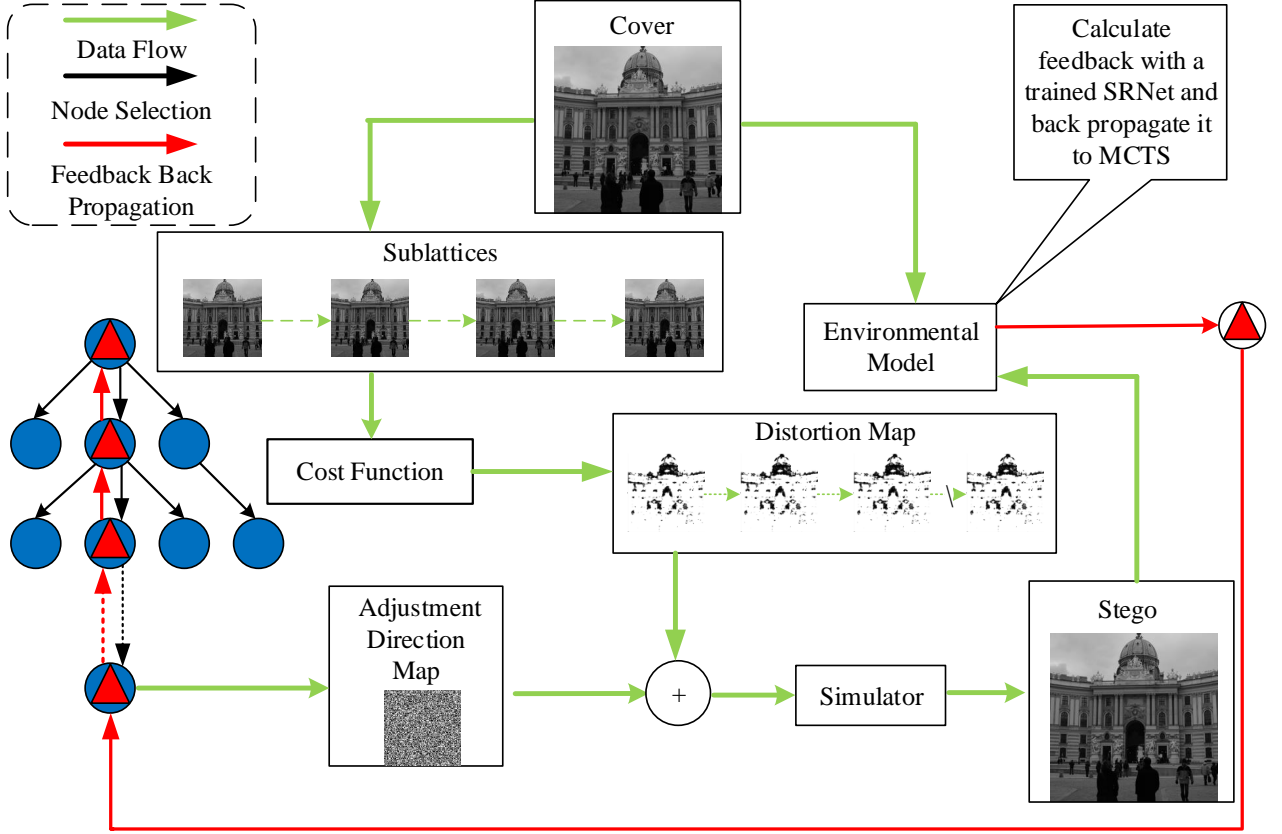


Fig. 1: The overall structure of MCTSteg. It first divides cover image into four sublattice, then embeds and updates them in turns according to distortion which has been adjusted by the search result of MCTS tree. Later MCTSteg will calculate feedback with the help of environmental model and back propagate it to nodes in the search path. After all sublattices have been embedded, the stego image generated by MCTSteg can be obtained.

- 3) *Complexity*: The initial state in non-additive steganography is different among cover images because their distortion distributions vary, which means that we have to discuss individual distortion adjustment for each of them.

As a consequence of these difficulties, the goal of our proposed framework MCTSteg is not discovering the optimal distortion adjustment but defeating the well-trained environmental model, which is similar to adversarial examples [43]. Moreover, the game results are decided by the classification of environmental model, which solves the problem of game rules. However, considering the computational complexity, we do not use gradient to attack the environmental model but adapt the reinforcement learning theory and design a low-complexity reward function. The details of our framework will be discussed in the rest of Sect. III.

B. Element Definitions

Let ρ^- denote the embedding distortion matrix of -1 modifications and ρ^+ for $+1$ modifications. Equations 3

and 4 can be expressed in the matrix form:

$$\rho^+ = \rho^+ \omega^+ \quad (6)$$

$$\rho^- = \rho^- \omega^-, \quad (7)$$

where ω^+ and ω^- are the distortion adjustment coefficient matrices for ρ^+ and ρ^- , respectively. To obtain the values in ω^+ and ω^- , we define a distortion adjustment polarity matrix $\Gamma = (\gamma_{i,j})^{r \times l}$, where r and l are the dimensions and $\gamma_{i,j} \in \{0, +1, -1\}$ in ternary embedding. Therefore, ω^+ and ω^- are expressed as:

$$\omega_{i,j}^+ = 1/\alpha \quad (\text{in which case } \gamma_{i,j} = 1) \quad (8)$$

$$\omega_{i,j}^- = \begin{cases} 1/\alpha & \gamma_{i,j} = -1 \\ \omega_{i,j}^+ & \gamma_{i,j} = 0. \end{cases} \quad (9)$$

As Γ decides distortion adjustment, we take MCTS into consideration because it can search the optimal sample in the distribution space of Γ . Before presenting the search process, we first define the following reinforcement learning elements to build the theoretical basis of MCTS tree:

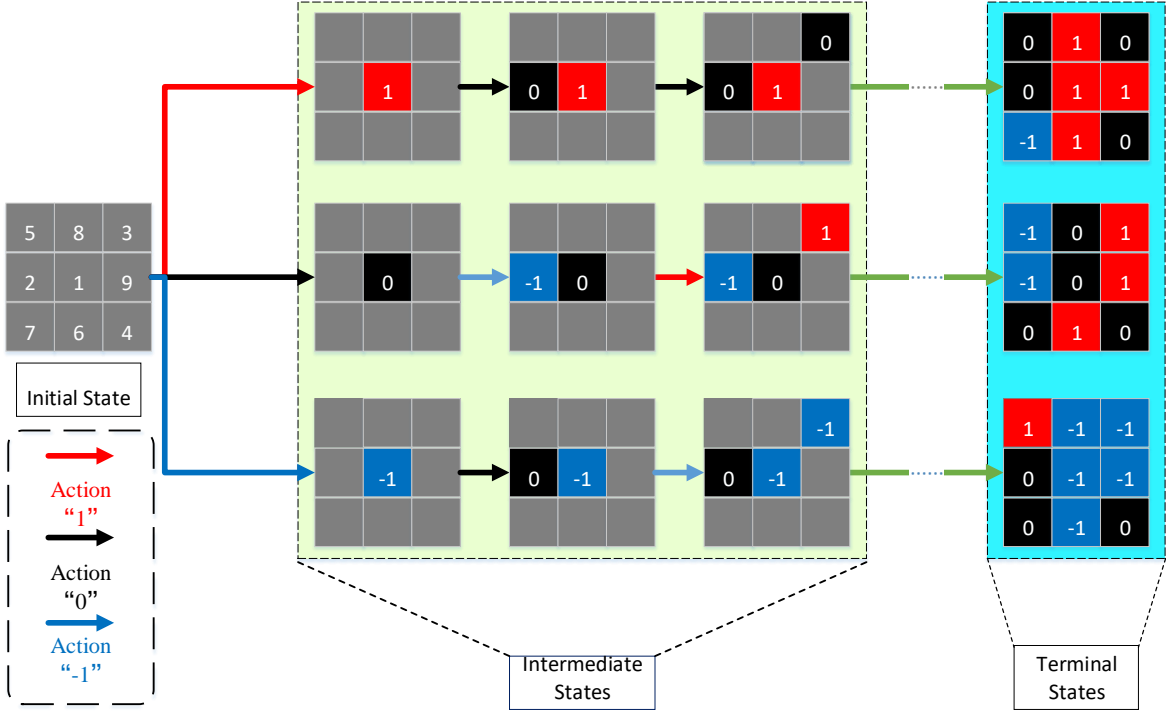


Fig. 2: An example of state transfer. The numbers in the initial state are distortion adjustment order. The red arrow represents for action “1” while black arrow is for “0” and blue arrow is for “-1”. An action is taken means that the value of corresponding elements of Γ will be changed.

- *States*: The set of states is denoted by Γ , which acts as parameter of tree nodes in MCTS. Specifically, we define Γ^0 for the initial state as:

$$\Gamma^0 = \{\gamma_{i,j} = 0 \mid \forall (i,j) \in \{1, \dots, r\} \times \{1, \dots, l\}\}, \quad (10)$$

where ρ^+ equals ρ^- at the initial state. We also define Γ^T for the terminal state, where $\{\gamma_{i,j} \mid \forall (i,j) \in \{1, \dots, r\} \times \{1, \dots, l\}\}$ have been assigned according to the search result of MCTS. An example procedure of transferring from the initial state to the terminal state is illustrated in Fig. 2.

- *Actions*: An action a takes one value in $\{-1, 0, +1\}$. Taking an action a means that the value of $\gamma_{i,j}$ will be changed to a based on selection policies, corresponding to node selection in MCTS. The illustration of action is also shown in Fig. 2.
- *Feedbacks*: As a zero-sum game, the feedback in non-additive steganography can only be determined until we attain Γ^T . The most common way to obtain feedbacks of intermediate states is using the same feedback of Γ^T . To evaluate the security performance of samples generated by MCTSteg, we design a reward function using the classification confidence. Let $f(\cdot)$ denote the well-trained environmental model and $f_c(\cdot)$ represent the confidence of $f(\cdot)$ to classify the input as cover.

The reward feedback R is calculated by:

$$R = f_c(M) - f_c(Y), \quad (11)$$

where M is the sample generated by MCTSteg, Y is the stego image used to attain security performance baseline. $f(\cdot)$ can roughly reflect the security performance of its inputs. Therefore if M can more effectively resist against the environmental model (i.e., R is positive), M will achieve better security performance compared with Y . If not (i.e., R is negative), M is worse. Theoretically, the better the environmental model we adopt, the values of R is closer to its actual distribution, which can help MCTSteg achieve better security performance.

In Sect. III-C, we will present how to utilize these elements defined above to build MCTSteg.

C. Overall Framework

Our proposed MCTSteg is composed of MCTS and a steganalyzer-based environmental model. The MCTS adjusts embedding distortion while the environmental model outputs the corresponding feedback introduced in Sect. III-B. The training of MCTSteg is similar to learn to defeat the environmental model. To do this, MCTS has to develop its strategies based on the corresponding environmental model’s feedback and try to attain global optimal search result.

MCTS has a trigeminal-tree structure, which is decided by the number of action types. The tree node has seven parameters:

- n : Visiting counts
- r : Cumulative reward
- p : Parent node
- lc : Left child
- mc : Middle child
- rc : Right child
- d : Adjustment order
- Γ : Distortion adjustment polarity matrix

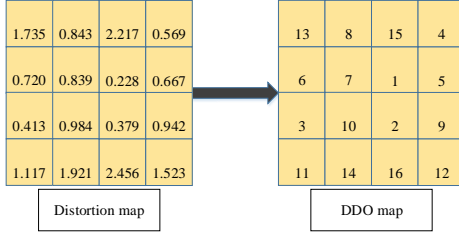


Fig. 3: The left matrix represents for a distortion map and the elements of DDO map is the descending order of distortion map.

During the search process, MCTSteg will sequentially make decisions until attaining terminal state. Each decision decides the distortion adjustment polarity of one specific pixel. Meanwhile, the nodes of MCTS in upper layers are visited more frequently, so their statistics are closer to actual distributions. Therefore, we design a new adjustment strategy called **distortion descending order (DDO)**. Firstly the pixels are sorted by their cost in descending order. Then we adjust distortion in that order. For example, in MCTSteg, pixels with lower cost are processed in upper layers while pixels with higher cost are processed in lower layers. Thus MCTSteg is more likely to process the pixels with lower cost, which effectively improves security performance.

Based on non-additive steganography, we design Algorithm 1 and Algorithm 2, which can be summarized as following workflow:

- 1) *Setup*: Let X denote the cover image. MCTSteg initializes the stego image $Y = X$, decomposes Y into N sublattices, and divides the embedding message into N segments. Let S_t denote the t -th sublattice, M_t denote the t -th segment, and Y_t denote partially embedded Y where S_1, \dots, S_{t-1} have been embedded. MCTSteg embeds S_1 with M_1 and goes to *Distortion Update* with $t = 1$.
- 2) *Distortion Update*: MCTSteg increases t by one. If $t > N$, it outputs Y_t as final stego images. Otherwise, it computes distortion based on Y_{t-1} with a cost function such as HILL and S(J)-UNIWARD and goes to *Sample Selection*.
- 3) *Sample Selection*: MCTSteg runs *Distortion Adjustment* within the computational budget and selects

Algorithm 1 Modules for MCTSteg

```

1: function GETCOORDINATE( $d$ )
2:    $x \leftarrow d / l$ ,  $y \leftarrow d \bmod l$ 
3:   return  $(x, y)$ 
4: end function
5: function BESTCHILD( $v$ )
6:    $C \leftarrow$  child set of  $v$ 
7:    $v' \leftarrow \arg \max_{c \in C} \text{UCTScore}(c)$ 
8:    $v'.n \leftarrow v'.n + 1$ 
9:   return  $v'$ 
10: end function
11: function BACKPROPAGATE( $v$ )
12:   Calculate  $R$  using Equation 11
13:   while  $v$  is not root node do
14:      $v.r \leftarrow v.r + R$ ,  $v \leftarrow v.p$ 
15:   end while
16: end function
17: function RANDOMSEARCH( $v$ )
18:   while  $v$  is not a leaf node do
19:     Randomly select an untried action  $a \in A(v)$ 
20:     Create a new node  $v'$ 
21:      $(x, y) \leftarrow \text{GETCOORDINATE}(v'.d)$ 
22:      $v'.p \leftarrow v$ ,  $v'.d \leftarrow v.d + 1$ ,  $v'.\Gamma \leftarrow v.\Gamma$ 
23:      $v'.\gamma_{x,y} \leftarrow a$ 
24:     if  $a = -1$  then
25:        $v.lc \leftarrow v'$ 
26:     else if  $a = 0$  then
27:        $v.mc \leftarrow v'$ 
28:     else
29:        $v.rc \leftarrow v'$ 
30:     end if
31:      $v \leftarrow v'$ 
32:   end while
33:   return  $v$ 
34: end function
35: function SEARCH( $v$ )
36:   while  $v$  is fully expanded do
37:      $v \leftarrow \text{BESTCHILD}(v)$ 
38:   end while
39:   if  $v$  is not a leaf node then
40:      $v \leftarrow \text{RANDOMSEARCH}(v)$ 
41:   end if
42:   return  $v$ 
43: end function

```

the Y_t^{tmp} with the highest R as Y_t .

- 4) *Distortion Adjustment*: MCTSteg executes the *search function* in Algorithm 1 on S_t and obtains the distortion adjustment polarity matrix Γ . It then embeds M_t into S_t according to the distortion adjusted by Γ , updates temporary stego Y_t^{tmp} with S_t , and executes the *backpropagate function* in Algorithm 1.

Inside the *search function*, we adopts UCT strategy for nodes that have been fully expanded (i.e., all of three child nodes including left child, middle child, and right child have

been visited) and random search for nodes that have not been fully expanded. For *backpropagate function*, MCTSteg will recursively accumulate the feedback to each node in the search path.

In Algorithm 2, the computational budget is designed based on the goal of the reinforcement learning paradigm, which is to achieve the highest total reward. The reward value is decided by R of every search result and the total search times. Therefore, we set up two computational budgets. The first one corresponds to R . If Y_t^{tmp} is classified as cover by the environmental model with confidence over 98%, then MCTS is considered to have found the highest R corresponding to the globally optimal result for S_t . It is worthless to continue search so we can stop *Distortion Adjustment* in advance. The second computational budget considers the time cost. We set a maximum search count for each sublattice. If the number of *Distortion Adjustment* executions reaches the maximum search count, we choose the Y_t^{tmp} with the highest R as the globally optimal result for S_t .

Algorithm 2 MCTSteg Algorithm

Require: Cover X , Message D
Require: Environmental Model R

- 1: **function** MAIN(X, M, R)
- 2: $Y \leftarrow X, t \leftarrow 1, Y_t \leftarrow Y$
- 3: Compute ρ^+ and ρ^- with the cost function
- 4: $Z \leftarrow \text{SIMULATOR}(X, \rho^+, \rho^-, M)$
- 5: $S_1 \leftarrow \text{SIMULATOR}(S_1, \rho^+, \rho^-, M_1)$
- 6: Update Y_2 with S_1
- 7: **while** $t \leq N$ **do**
- 8: $t \leftarrow t + 1$
- 9: Create root node V^0 with state Γ^0
- 10: Get sublattice S_t from Y and M_t from M
- 11: $R_{\text{top}} \leftarrow 0, Y_t^{\text{tmp}} \leftarrow Y_t$
- 12: **while** within the computational budget **do**
- 13: $V^T \leftarrow \text{SEARCH}(V^0)$
- 14: Get Γ^T from V^T
- 15: Adjust ρ^+ and ρ^- according to Γ^T
- 16: $S_t^{\text{tmp}} \leftarrow \text{SIMULATOR}(S_t, \rho^+, \rho^-, D_t)$
- 17: Update Y_t^{tmp} with S_t^{tmp}
- 18: $R \leftarrow f_c(Y_t^{\text{tmp}}) - f_c(Z)$
- 19: BACKPROPAGATE(V^T, R)
- 20: **if** $R_{\text{top}} < R$ **then**
- 21: $R_{\text{top}} \leftarrow R$
- 22: $Y_t \leftarrow Y_t^{\text{tmp}}$
- 23: **end if**
- 24: **end while**
- 25: **end while**
- 26: **end function**

IV. EXPERIMENTS

We first give the experimental setup including datasets, environmental model, and steganographic and steganalysis methods. Then we tune the hyperparameters of MCTSteg

and compare MCTSteg and non-additive steganography in spatial and JPEG domains. Finally, we adopt ALASKA-v2 to compare MCTSteg and state-of-the-art machine learning-based steganographic methods, which gives a more comprehensive conclusion. The source codes and auxiliary materials are available for download from GitHub ¹.

A. Experimental Setup

1) *Dataset for the Environmental Model:* SZUBase has 40,000 512×512 full-resolution raw images. These images were collected by our laboratory, and converted with the same script of BOSSBase [44]. Due to copyright protection, they are not publicly available yet.

To protect the independence of training and testing datasets, prior research (including ASDL-GAN [36], UT-GAN [37], and SPAR-RL [38]) utilizes SZUBase to train the steganalyzer and evaluates the security performance with other datasets. Therefore, we also adopt SZUBase for MCTSteg to train a SRNet [34] based environmental model. After scaling down to 256×256 with “imresize” Matlab function, 38,000 cover-stego image pairs are used for training while the remaining 2,000 are used for validation. The stego images are generated by arbitrary steganography such as HILL [6] and JUNIWARD [5]. Specifically, in the JPEG domain, all images are decompressed without integer rounding. We train SRNet for 400k iterations with an initial learning rate of $r_1 = 0.001$. Then the learning rate is decreased to $r_2 = 0.0001$ for an additional 100k iterations, which is the same as the setting of Boroumand et al. [34]. Finally, we select the trained model with the highest validation accuracy as our environmental model.

2) *Datasets for Performance Verification:* To compare MCTSteg with other state-of-the-art steganography, we use three datasets of BOSSBase v1.10 [44], BOWSD2 [45], and ALASKA2 [46]. Both BOSSBase and BOWSD2 are composed of 10,000 grayscale images with size 512×512 and “pgm” format. Due to the limited memory of our GPU (Tesla P100), we use “imresize” in Matlab with default settings to scale down those images to 256×256. For the JPEG domain, we use “imwrite” in Matlab to transform the format from “pgm” to “jpg” with QF=75. The ALASKA2 dataset contains 80,000 images of various sizes and formats. We use the 256×256 size in both JPEG and spatial domains.

3) *Steganographic Method:* To prove that our MCTSteg can improve the security performance of additive steganography, we choose basic cost functions including S-(J)UNIWARD [5] and HILL [6]. Then we compare MCTSteg and four state-of-the-art non-additive steganographic frameworks, including CMD [11] and Synch [12] for the spatial domain, and BBC [13] and BBM [15] for the JPEG domain.

4) *Steganalyzer:* We use four state-of-the-art steganalyzers in JPEG and spatial domains for a more comprehensive comparison. They are based on either hand-crafted

¹<https://github.com/tansq/MCTSteg>

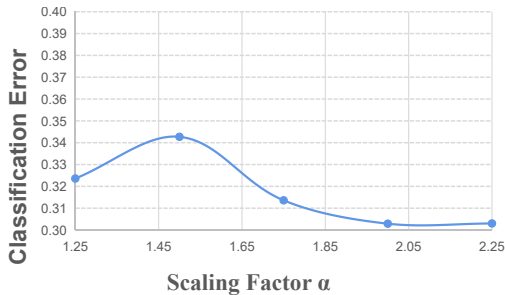


Fig. 4: Classification error rates (maxSRMd2) of MCTSteg with different values of scaling factor α .

features or CNN structures. For hand-crafted feature-based steganalyzers, we adopt SRM [20], maxSRMd2 [47], and GFR [48]. For CNN structure-based steganalyzers, we adopt SRNet [34], the most powerful one so far.

B. Hyperparameter Tuning

There are two major hyperparameters in MCTSteg, the maximum search count N and the scaling factor α . N balances the security performance and training time. It is empirically set to 128. The scaling factor α adjusts distortion distribution as Equations 8 and 9 show. With a payload of 0.4bpp, we use *BOSSBase* and maxSRMd2 to search for the best value of α in the spatial domain and find that the minimum classification error rate is achieved when $\alpha = 1.5$ (Fig. 4). Therefore, for the rest of Sect. IV, we adopt the N of 128 and the α of 1.5.

C. Visualizing Embedding Modification

To make a visual comparison between the modification maps of different steganographic methods, we sample a cover image from *BOSSBase* v1.10 as Fig. 5(a) shows, which contains smooth regions, edges, and textured regions. Fig. 5(b) is cropped from Fig. 5(a) where the red rectangles denotes the cropped area. For better visual effects, we embed the cover image with payload of 0.4 bits per pixel (bpp) by using additive cost functions including SUNIWARD, HILL and non-additive frameworks including CMD, MCTSteg. The modification maps are shown in Fig. 5 (c) to (h). We can see that all steganographic methods are prefer to embed message into the texture regions. However, the embedding modifications of MCTSteg are more concentrated into the center texture regions. On the contrary, for the boundaries between smooth regions and texture regions, there are fewer modifications of MCTSteg. Actually, manual strategies such as CMD will reduce the costs of pixels at those boundaries, which causes some pixels at the smooth regions are more likely to be modified. Moreover, the distributions of embedding modification between CMD and MCTSteg are obviously different, which means that the distortion adjustment strategies between MCTSteg and CMD are also different. Therefore, without human intervention, MCTSteg successfully develop its own novel strategies.

D. Statistical Analysis

To analyze statistically, we calculate the change rates of these methods and then adopt FCC [11] as an evaluation metric to compute the average frequency of occurrences in the row/column direction for consecutive positive/negative changes. The n -th order FCC, denoted as $F(n)$, is defined by:

$$F(n) = \frac{1}{4}(H(n, 1) + H(n, -1) + V(n, 1) + V(n, -1)), \quad (12)$$

where

$$H(n, k) = \frac{\sum_{i=1}^{n_1} \sum_{j=1}^{n_2-n+1} (\delta(d_{i,j-k}) \dots \delta(d_{i,j+n-k}))}{n_1(n_2-n+1)} \quad (13)$$

$$V(n, k) = \frac{\sum_{i=1}^{n_1-n+1} \sum_{j=1}^{n_2} (\delta(d_{i,j-k}) \dots \delta(d_{i+n,j-k}))}{(n_1-n+1)n_2}, \quad (14)$$

where $\delta(\cdot)$ is an impulse function and d is a modification map.

The FCC scores and change rates are shown in Tab. I. MCTSteg's second- to fourth-order FCC scores are much higher than those of other methods. MCTSteg's fourth-order FCC score is even more than twice of CMD's. The results indicate that there is a similarity between the distortion adjustment strategy of MCTSteg and CMD. Meanwhile, the value of α in MCTSteg is much smaller than that in CMD, which means that our framework has successfully learned the hidden rules in SRNet and developed its embedding strategy. Moreover, MCTSteg achieves the lowest change rate among these methods, which indicates better security performance. Therefore, in the next section, we compare the security performance of different steganographic methods.

E. Comparison of state-of-the-art Non-additive Methods

To compare security performance of different steganographic methods, we adopts detection error rate P_E on testing set, which is calculated by the false alarm rate P_{FA} and the missed detection rate P_{MD} as follows:

$$P_E = \min_{P_{FA}} \frac{1}{2}(P_{FA} + P_{MD}). \quad (15)$$

In the spatial domain, we adopt SUNIWARD and HILL as basic additive cost functions and compare security performance between Synch, CMD, and MCTSteg with payloads of 0.2 and 0.4bpp. Detected by SRM and maxSRMd2, the results on *BOSSBase* are shown in Tab. II.

From Tab. II, we can see that MCTSteg achieves substantial improvement based on both SUNIWARD and HILL. Under the payload of 0.4bpp and detected by maxSRMd2, the improvement of our MCTSteg is **15.29%**, which is **3.31%** higher than that of CMD. As for SRM, the performance margin between MCTSteg and other enhancement methods is also significant.

To compare security performance against recent CNN-based steganalyzers, we follow the setting of SRNet [34] and additionally include *BOWS2* into our experiment to expand the size of the dataset. For the combined *BOSSBase+BOWS2*, we randomly split it into three sets with

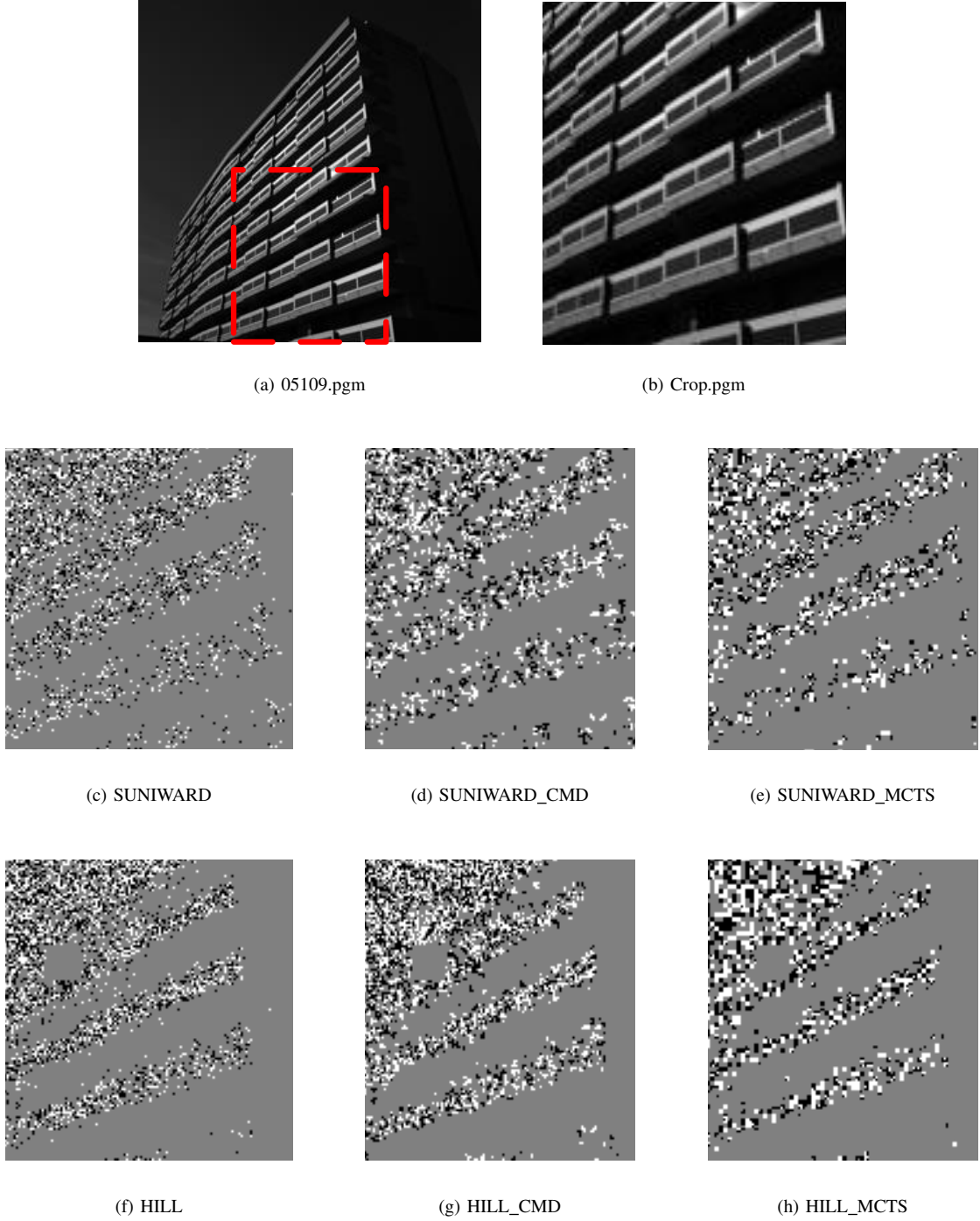


Fig. 5: (a) is a sample cover image where the area in the red rectangles is cropped into (b). (c) to (h) are the modification maps, where white pixels represent the modification of “+1” and dark pixels represent the modification of “-1”. Due to possibly low printing resolution, readers are encouraged to zoom in the figures on a computer screen for better clarity.

14,000, 1000, and 5000 examples for training, validation, and testing, respectively. Then we train SRNet for 500k iterations with the same settings in Boroumand et al. [34] and present the results in Tab. III. All of these non-additive steganographic frameworks increase the detection error rates against SRNet. MCTSteg achieves the highest improvement

of **9.79%** over the original HILL at the payload of 0.2bpp.

In the JPEG domain, we adopt JUNIWARD as basic additive steganography and compare security performance among MCTSteg, BBC [13], and BBC-BBM (i.e., the combination of BBC and BBM [15]) with QF=75, because Wang et al. [15] report that BBC-BBM achieves better security

TABLE I: Statistical analysis of different steganographic methods on *BOSSBase* with payload 0.4bpp

Methods	α	Change Rates	FCC (2nd Order)	FCC (3rd Order)	FCC (4th Order)
HILL	N/A	9.60%	0.640%	0.113%	0.022%
HILL_CMD	9	12.4%	1.805%	0.461%	0.101%
HILL_MCTSteg	1.5	9.06%	2.146%	0.509%	0.261%

TABLE II: P_E of different steganographic methods against SRM and maxSRMd2 in the spatial domain on *BOSSBase*

Steganography		SRM		maxSRMd2	
		0.2bpp	0.4bpp	0.2bpp	0.4bpp
SUNIWARD	Baseline	33.71%	21.97%	30.42%	20.49%
	Synch	39.98%(↑ 6.27%)	30.14%(↑ 8.17%)	40.26%(↑ 9.84%)	30.22%(↑ 9.73%)
	CMD	40.61%(↑ 6.90%)	30.58%(↑ 8.61%)	40.74%(↑ 10.32%)	30.65%(↑ 10.16%)
	MCTSteg	41.87%(↑ 8.16%)	34.42%(↑ 12.45%)	41.60%(↑ 11.18%)	34.27%(↑ 13.78%)
HILL	Baseline	38.40%	27.93%	32.94%	23.88%
	Synch	43.11%(↑ 4.71%)	35.29%(↑ 7.36%)	43.08%(↑ 10.14%)	35.23%(↑ 11.35%)
	CMD	43.51%(↑ 5.11%)	35.95%(↑ 8.02%)	43.34%(↑ 10.40%)	35.86%(↑ 11.98%)
	MCTSteg	44.01%(↑ 5.61%)	39.33%(↑ 11.40%)	43.67%(↑ 10.73%)	39.17%(↑ 15.29%)

TABLE III: P_E of different steganographic methods against SRNet on *BOSSBase+BOWS2* in the spatial domain

Framework	Baseline	Synch	CMD	MCTSteg
Payload	0.2bpp			
S-UNIWARD	20.90%	28.31%(↑ 7.41%)	28.45%(↑ 7.95%)	29.81%(↑ 8.91%)
HILL	23.53%	32.17%(↑ 8.64%)	32.29%(↑ 8.76%)	33.32%(↑ 9.79%)
Payload	0.4bpp			
S-UNIWARD	10.15%	16.20%(↑ 6.05%)	16.23%(↑ 6.08%)	16.57%(↑ 6.42%)
HILL	14.14%	21.93%(↑ 7.79%)	22.14%(↑ 8.00%)	22.74%(↑ 8.60%)

performance than either BBC or BBM.

For traditional hand-crafted feature-based steganalyzers, we select GFR and its results are shown in Tab. IV. Under the payload of 0.4BPNZAC, MCTSteg achieves the highest security performance which is **3.7%** higher than JUNIWARD.

For SRNet, we also use the same settings in Boroumand et al. [34] and show the results in Tab. V. The gaps in detection error rates between MCTSteg and other methods are substantial. For example, MCTSteg’s improvement is **7.78%** while BBC-BBM’s is **-5.26%** with a payload of 0.2BPNZAC.

Overall, our proposed MCTSteg achieves the best security performance against both hand-crafted feature-based and deep learning-based steganalyzers. In the next section, we compare the security performance between MCTSteg and other state-of-the-art machine learning-based steganographic methods.

F. Comparison with Machine Learning-Based Methods

In this section, we adopt ASDL-GAN [49], UT-GAN [37], and SPAR-RL [38] for comparison, while HILL is the base-

line. Considering the time-cost problem, we use SRM and maxSRMd2 to evaluate the security performance of these methods with payloads of 0.2 and 0.4bpp. The ALASKA-v2 dataset is split into a training set and a test set of the same size (40,000 either). The results are shown in Tab. VI.

We can see that under the payload of 0.4bpp and detected by SRM and maxSRMd2, the security performance of our method is **5.34%** and **6.42%** higher than HILL respectively. For other methods, ASDL-GAN is obviously worse than HILL, UT-GAN and SPAR-RL are better than HILL but worse than MCTSteg.

As for the payload of 0.2bpp, MCTSteg achieves **47.61%** and **47.89%** error rate, which means that the classification result of SRM and maxSRMd2 is close to random prediction. Meanwhile the security performance of ASDL-GAN is lower than HILL while UT-GAN and SPAR-RL achieve comparable security performance of HILL. Therefore, from Tab. VI, we get a conclusion that MCTSteg achieves the best security performance among all the machine learning-based steganographic methods.

TABLE IV: P_E of different steganographic methods against GFR on *BOSSBase* in the JPEG domain with QF=75

Framework	Baseline	BBM	BBC-BBM	MCTSteg
Payload	0.2BPNZAC			
J-UNIWARD	39.71%	40.62%(↑ 0.91%)	32.39%(↓ -7.32%)	40.84%(↑ 1.13%)
Payload	0.4BPNZAC			
J-UNIWARD	25.39%	27.91%(↑ 2.52%)	28.71%(↑ 3.32%)	29.12%(↑ 3.70%)

TABLE V: P_E of different steganographic methods against SRNet on *BOSSBase+BOWS2* in the JPEG domain with QF=75

Framework	Baseline	BBM	BBC-BBM	MCTSteg
Payload	0.2BPNZAC			
J-UNIWARD	18.89%	23.50%(↑ 4.61%)	13.63%(↓ -5.26%)	26.67%(↑ 7.78%)
Payload	0.4BPNZAC			
J-UNIWARD	6.70%	8.37%(↑ 1.67%)	9.10%(↑ 2.40%)	13.47%(↑ 6.77%)

TABLE VI: P_E of different steganographic methods against SRM and maxSRMd2 on ALASKA-v2 in the spatial domain

Steganalyzer	Steganographic Method	0.2 bpp	0.4 bpp
SRM	HILL	45.04%	39.23%
	ASDL-GAN	41.24% (↓ 3.80%)	36.95% (↓ 2.28%)
	UT-GAN	44.87% (↓ 0.17%)	39.31% (↑ 0.08%)
	SPAR-RL	45.13% (↑ 0.09%)	40.63% (↑ 1.40%)
	MCTSteg_HILL	47.61%(↑ 2.57%)	44.57%(↑ 5.34%)
maxSRMd2	HILL	44.53%	38.55%
	ASDL-GAN	41.85% (↓ 2.68%)	36.83% (↓ 1.72%)
	UT-GAN	44.76% (↑ 0.23%)	40.29% (↑ 1.74%)
	SPAR-RL	44.28% (↓ 0.25%)	41.36% (↑ 2.81%)
	MCTSteg_HILL	47.89%(↑ 3.34%)	44.97%(↑ 6.42%)

V. CONCLUSIONS AND FUTURE WORK

In this paper we propose MCTSteg, the first automatic non-additive steganographic framework based on reinforcement learning paradigm. It is composed of a MCTS based non-additive steganographer and a steganalyzer-based environmental model. The major contributions are as follows:

- In order to remove the restrictions in existing non-additive steganography such as confine of a specific domain and dependence on professional knowledge, we have proposed the first reported universal automatic non-additive steganographic distortion learning framework, which can work in both spatial and JPEG domain. It aims at automatically adjusting distortion distribution without human intervention. Furthermore, a new distortion adjustment strategy has been proposed which helps MCTSteg achieve better security performance.
- To model the game between a non-additive steganographer and a target steganalyzer, we have designed fundamental reinforcement learning elements including state, action, reward function, and environmental model. Based on the above elements, our proposed MCTSteg

can effectively combine the search space of MCTS with the distortion metric of the underlying distortion minimization framework.

- Extensive experimental results have demonstrated that MCTSteg steadily outperforms the state of the art by a clear margin in different benchmark datasets, which confirms that a more secure distortion adjustment strategy has been learned by MCTSteg.

Our future work will focus on the following aspects: (1) we will try to design a policy network for learning distortion adjustment policies based on the samples generated by MCTSteg; (2) we will try to increase the types of actions in MCTSteg and build a more elastic framework.

REFERENCES

- [1] B. Li, J. He, J. Huang, and Y. Q. Shi, "A survey on image steganography and steganalysis," *Journal of Information Hiding and Multimedia Signal Processing*, vol. 2, no. 2, pp. 142–172, 2011.
- [2] J. Fridrich and T. Filler, "Practical methods for minimizing embedding impact in steganography," *Security, Steganography, and Watermarking of Multimedia Contents IX*, vol. 6505, p. 650502, 2007.

- [3] T. Pevný, T. Filler, and P. Bas, "Using high-dimensional image models to perform highly undetectable steganography," in *Proceedings of the 12th international conference on Information hiding*, 2010, pp. 161–177.
- [4] V. Holub and J. Fridrich, "Designing steganographic distortion using directional filters," in *IEEE International Workshop on Information Forensics & Security*, 2012.
- [5] V. Holub, J. Fridrich, and T. Denemark, "Universal distortion function for steganography in an arbitrary domain," *Eurasip Journal on Information Security*, vol. 2014, no. 1, pp. 1–13, 2014.
- [6] B. Li, M. Wang, J. Huang, and X. Li, "A new cost function for spatial image steganography," in *2014 IEEE International Conference on Image Processing (ICIP)*, 2015.
- [7] W. Zhou, W. Zhang, and N. Yu, "A new rule for cost reassignment in adaptive steganography," *IEEE Transactions on Information Forensics & Security*, vol. 12, no. 11, pp. 2654–2667, 2017.
- [8] L. Guo, J. Ni, and Y. Q. Shi, "Uniform embedding for efficient jpeg steganography," *IEEE Transactions on Information Forensics & Security*, vol. 9, no. 5, pp. 814–825, 2014.
- [9] S. Kouider, M. Chaumont, and W. Puech, "Adaptive steganography by oracle (ASO)," in *2013 IEEE International Conference on Multimedia and Expo (ICME)*, 2013, pp. 1–6.
- [10] T. Filler and J. Fridrich, "Gibbs construction in steganography," *IEEE Transactions on Information Forensics & Security*, vol. 5, no. 4, pp. 705–720, 2010.
- [11] B. Li, M. Wang, X. Li, S. Tan, and J. Huang, "A strategy of clustering modification directions in spatial image steganography," *IEEE Transactions on Information Forensics & Security*, vol. 10, no. 9, pp. 1905–1917, 2015.
- [12] T. Denemark and J. Fridrich, "Improving steganographic security by synchronizing the selection channel," in *Proceedings of the 3rd ACM Workshop on Information Hiding and Multimedia Security*, 2015, pp. 5–14.
- [13] W. Li, W. Zhang, K. Chen, W. Zhou, and N. Yu, "Defining joint distortion for JPEG steganography," in *Proceedings of the 6th ACM Workshop on Information Hiding and Multimedia Security*, 2018, pp. 5–16.
- [14] Y. Wang *et al.*, "BBC++: Enhanced block boundary continuity on defining non-additive distortion for jpeg steganography," *IEEE Transactions on Circuits and Systems for Video Technology*, pp. 1–1, 2020.
- [15] Y. Wang, W. Zhang, W. Li, and N. Yu, "Non-additive cost functions for JPEG steganography based on block boundary maintenance," *IEEE Transactions on Information Forensics & Security*, vol. 16, pp. 1117–1130, 2020.
- [16] W. Zhang, S. Wang, and X. Zhang, "Improving embedding efficiency of covering codes for applications in steganography," *IEEE Communications Letters*, vol. 11, no. 8, pp. 680–682, 2007.
- [17] W. Zhang, X. Zhang, and S. Wang, "Near-optimal codes for information embedding in gray-scale signals," *IEEE Transactions on Information Theory*, vol. 56, no. 3, pp. 1262–1270, 2010.
- [18] T. Filler, J. Judas, and J. Fridrich, "Minimizing additive distortion in steganography using syndrome-trellis codes," *IEEE Transactions on Information Forensics & Security*, vol. 6, no. 3, pp. 920–935, 2011.
- [19] W. Li, W. Zhang, L. Li, H. Zhou, and N. Yu, "Designing near-optimal steganographic codes in practice based on polar codes," *IEEE Transactions on Communications*, vol. 68, no. 7, pp. 3948–3962, 2020.
- [20] J. Fridrich and J. Kodovsky, "Rich models for steganalysis of digital images," *IEEE Transactions on Information Forensics & Security*, vol. 7, no. 3, pp. 868–882, 2012.
- [21] T. Denemark, V. Sedighi, V. Holub, R. Cogranne, and J. Fridrich, "Selection-channel-aware rich model for steganalysis of digital images," in *IEEE Workshop on Information Forensic & Security*, 2014.
- [22] W. Tang, H. Li, W. Luo, and J. Huang, "Adaptive steganalysis based on embedding probabilities of pixels," *IEEE Transactions on Information Forensics & Security*, vol. 11, no. 4, pp. 734–745, 2016.
- [23] S. Tan, H. Zhang, B. Li, and J. Huang, "Pixel-decimation-assisted steganalysis of synchronize-embedding-changes steganography," *IEEE Transactions on Information Forensics & Security*, vol. 12, no. 7, pp. 1658–1670, 2017.
- [24] B. Li, Z. Li, S. Zhou, S. Tan, and X. Zhang, "New steganalytic features for spatial image steganography based on derivative filters and threshold LBP operator," *IEEE Transactions on Information Forensics & Security*, vol. 13, no. 5, pp. 1242–1257, 2017.
- [25] J. Kodovsky, J. Fridrich, and V. Holub, "Ensemble classifiers for steganalysis of digital media," *IEEE Transactions on Information Forensics & Security*, vol. 7, no. 2, pp. 432–444, 2012.
- [26] S. Tan and B. Li, "Stacked convolutional auto-encoders for steganalysis of digital images," in *Proc. Asia-Pacific Signal and Information Processing Association Annual Summit and Conference (APSIPA'2014)*, 2014, pp. 1–4.
- [27] G. Xu, H. Z. Wu, and Y. Q. Shi, "Structural design of convolutional neural networks for steganalysis," *IEEE Signal Processing Letters*, vol. 23, no. 5, pp. 708–712, 2016.
- [28] Y. Qian, J. Dong, W. Wang, and T. Tan, "Deep learning for steganalysis via convolutional neural networks," in *Proc. IS&T/SPIE Electronic Imaging 2015 (Media Watermarking, Security, and Forensics)*, 2015, pp. 94 090J–1–94 090J–10.
- [29] M. Yedroudj, F. Comby, and M. Chaumont, "Yedroudj-net: An efficient CNN for spatial steganalysis," in *2018 IEEE International Conference on Acoustics, Speech and Signal Processing (ICASSP)*. IEEE, 2018, pp. 2092–2096.
- [30] J. Ye, J. Ni, and Y. Yi, "Deep learning hierarchical representations for image steganalysis," *IEEE Transactions on Information Forensics & Security*, vol. 12, no. 11, pp. 2545–2557, 2017.
- [31] M. Chen, V. Sedighi, M. Boroumand, and J. Fridrich, "JPEG-phase-aware convolutional neural network for steganalysis of JPEG images," in *Proc. 5th ACM Information Hiding and Multimedia Security Workshop (IH&MMSec'2017)*, 2017, pp. 75–84.
- [32] G. Xu, "Deep convolutional neural network to detect J-UNIWARD," in *Proc. 5th ACM Information Hiding and Multimedia Security Workshop (IH&MMSec'2017)*, 2017, pp. 67–73.
- [33] J. Zeng, S. Tan, B. Li, and J. Huang, "Large-scale jpeg image steganalysis using hybrid deep-learning framework," *IEEE Transactions on Information Forensics & Security*, vol. 13, no. 5, pp. 1200–1214, 2018.
- [34] M. Boroumand, M. Chen, and J. Fridrich, "Deep residual network for steganalysis of digital images," *IEEE Transactions on Information Forensics & Security*, vol. 14, no. 5, pp. 1181–1193, 2018.
- [35] S. Tan *et al.*, "CALPA-NET: Channel-pruning-assisted deep residual network for steganalysis of digital images," *IEEE Transactions on Information Forensics & Security*, vol. 16, pp. 131–146, 2021.
- [36] W. Tang, S. Tan, B. Li, and J. Huang, "Automatic steganographic distortion learning using a generative adversarial network," *IEEE Signal Processing Letters*, vol. 24, no. 99, pp. 1547–1551, 2017.
- [37] J. Yang, D. Ruan, J. Huang, X. Kang, and Y.-Q. Shi, "An embedding cost learning framework using GAN," *IEEE Transactions on Information Forensics & Security*, vol. 15, pp. 839–851, 2019.
- [38] W. Tang, B. Li, M. Barni, J. Li, and J. Huang, "An automatic cost learning framework for image steganography using deep reinforcement learning," *IEEE Transactions on Information Forensics & Security*, vol. 16, pp. 952–967, 2020.
- [39] D. Silver *et al.*, "Mastering the game of Go with deep neural networks and tree search," *nature*, vol. 529, no. 7587, pp. 484–489, 2016.
- [40] —, "Mastering the game of Go without human knowledge," *nature*, vol. 550, no. 7676, pp. 354–359, 2017.
- [41] P. Auer, N. Cesa-Bianchi, and P. Fischer, "Finite-time analysis of the multiarmed bandit problem," *Machine learning*, vol. 47, no. 2-3, pp. 235–256, 2002.
- [42] C. B. Browne *et al.*, "A survey of monte carlo tree search methods," *IEEE Transactions on Computational Intelligence and AI in games*, vol. 4, no. 1, pp. 1–43, 2012.
- [43] A. Nguyen, J. Yosinski, and J. Clune, "Deep neural networks are easily fooled: High confidence predictions for unrecognizable images," in *Proceedings of the IEEE Conference on Computer Vision and Pattern Recognition*, 2015, pp. 427–436.
- [44] P. Bas, T. Filler, and T. Pevný, "'break our steganographic system': The ins and outs of organizing boss," in *Proceedings of the 13th International Conference on Information Hiding*, 2011.
- [45] P. Bas and T. Furon, "Break our watermarking system," <http://bows2.ec-lille.fr/>, accessed Mar. 18, 2021.
- [46] "ALASKA#2 steganalysis challenge," <https://alaska.utt.fr/>, accessed Mar. 18, 2021.
- [47] T. Denemark, V. Sedighi, V. Holub, R. Cogranne, and J. Fridrich, "Selection-channel-aware rich model for steganalysis of digital images," in *2014 IEEE International Workshop on Information Forensics and Security (WIFS)*. IEEE, 2014, pp. 48–53.
- [48] X. Song, F. Liu, C. Yang, X. Luo, and Y. Zhang, "Steganalysis of adaptive JPEG steganography using 2D Gabor filters," in *Proceedings*

of the 3rd ACM workshop on information hiding and multimedia security, 2015, pp. 15–23.

- [49] W. Tang, H. Li, W. Luo, and J. Huang, “Adaptive steganalysis based on embedding probabilities of pixels,” *IEEE Transactions on Information Forensics & Security*, vol. 11, no. 4, pp. 734–745, 2016.